https://doi.org/10.3311/PPch.43095

Periodica Polytechnica Chemical Engineering

Sustainable Deep Eutectic Solvent Modified Multi-Walled Carbon Nanotubes for Ibuprofen Removal from Pharmaceutical Effluents

Nagul Dev Selvanatrajan[1], Palani Ramasamay[1*]

[1] Department of Chemical Engineering, Hindusthan College of Engineering and Technology, Coimbatore, Tamilnadu 641032, India
[*] Corresponding author, e-mail: palani79@gmail.com

Received: 15 December 2025, Accepted: 23 February 2026, Published online: 20 April 2026

Abstract

The increasing occurrence of pharmaceutical residues such as ibuprofen in aquatic systems poses a growing environmental concern. In this study, oxidized multi-walled carbon nanotubes (MWCNTs) were functionalized using an ecofriendly deep eutectic solvent prepared from tetrabutylammonium bromide and glycerol. The modified nanotubes were thoroughly characterized and evaluated for their adsorption performance towards ibuprofen removal from aqueous media. Batch experiments were carried out to investigate the influence of pH, temperature and contact time. The process was optimized through response surface methodology (RSM), and the results were validated using an artificial neural network (ANN) model. Fourier transform infrared and field emission scanning electron microscope analyses verified the surface modification and morphological variation after deep eutectic solvent (DES) coating. Optimum adsorption occurred at 35 °C, pH 4 and 90 min, resulting in a removal efficiency 94.9%. The kinetic data followed the pseudo second order model (R^2 = 0.9715) and the Langmuir Isotherm gave the best fit with R^2 = 0.9602 and a capacity 86.2 mg/g). In addition, desorption studies demonstrated high regeneration efficiency (>96%), indicating that the adsorption process is largely reversible and that the DES-functionalized MWCNTs possess strong potential for repeated use in wastewater treatment applications. Both RSM and ANN predictions closely matched experimental outcomes (R^2 > 0.998), confirming their reliability. To the best of our knowledge, this is the first study that employs TBAB-glycerol DES functionalization of MWCNTs for ibuprofen removal combined with dual ANN-RSM modeling, demonstrating a uniquely green and high-efficiency adsorption system.

Keywords

deep eutectic solvent (DES), multi-walled carbon nanotubes (MWCNTs), ibuprofen, adsorption, response surface methodology, artificial neural network, pharmaceutical wastewater

1 Introduction

Ibuprofen, chemically identified as 2-(4-(2-methylpropyl) phenyl) propanoic acid, is a widely used non-steroidal anti-inflammatory drug (NSAID) owing to its effective analgesic, antipyretic, and inflammatory properties [1, 2]. Since its introduction in 1961, its widespread application in human and animal healthcare has led to its recognition as an emerging environmental contaminant of concern [3]. Ibuprofen reaches aquatic environments through several routes. The environment is affected not only by the improper disposal of unused medications and effluents discharged from pharmaceutical manufacturing units and healthcare facilities, but also by municipal wastewater, which contains significant amounts of pharmaceuticals originating from drugs that are only partially metabolized in humans and animals [4, 5]. Earlier investigations have reported the presence of ibuprofen in wastewater, surface water, and even in certain groundwater samples, with measured concentrations up to a few µg/L [1, 5].

The persistence of ibuprofen in aquatic environments raises ecological and toxicological concerns. Researchers have observed harmful effects on aquatic life, including reproductive and developmental abnormalities, DNA damage, and endocrine disruption in fish and invertebrates [3, 6]. From our own review of recent studies, it appears that conventional wastewater treatment plants (WWTPs) often fail to completely remove ibuprofen and its metabolites because of the its stability and hydrophobic nature (log $P \approx 3.97$, where P is the partition

Cite this article as: Selvanatrajan, N. D., Ramasamay, P. "Sustainable Deep Eutectic Solvent Modified Multi-Walled Carbon Nanotubes for Ibuprofen Removal from Pharmaceutical Effluents", Periodica Polytechnica Chemical Engineering, 2026. https://doi.org/10.3311/PPch.43095

coefficient) [4, 7]. Similar limitations of conventional treatment systems have been reported for other hydrophobic organic micropollutants, highlighting the necessity for advanced and more efficient treatment strategies to eliminate pharmaceutical contamination in aquatic systems [8].

Several treatment approaches have been investigated for the elimination of ibuprofen, including advanced oxidation process (AOPs) [9, 10], photocatalysis [11] and membrane filtration. However, in many practical cases, these techniques face challenges such as high operational costs and elevated energy demands, or the generation of toxic by-products [5]. Among the available methods, adsorption has emerged as a promising alternative owing to its operational simplicity, cost-effectiveness and high removal efficiency [12]. In this regard, carbon-based nanomaterials, particularly multi-walled carbon nanotubes (MWCNTs), have attracted substantial attention as advanced adsorbents due to their high specific surface area, well-developed pore structure, and favorable adsorption kinetics [12, 13]. Previous studies have demonstrated that MWCNT-based composites and functionalized carbon nanotubes (CNTs) exhibit excellent adsorption performance toward pharmaceutical contaminants, including acetaminophen and other aromatic drug molecules, primarily through hydrophobic interactions and π–π electron donor–acceptor interactions [14].

Surface functionalization of MWCNTs has been shown to significantly enhance their adsorption performance by improving dispersibility, introducing active functional groups, and strengthening adsorbate–adsorbent interactions [15].

In recent years, deep eutectic solvents (DESs) have gained significant attention as sustainable and eco-friendly alternatives to conventional organic ionic liquid solvents, finding various application, including material modification [15, 16]. DESs typically formed by combining a hydrogen bond acceptor (HBA), often a quaternary ammonium or phosphonium salt, with a hydrogen bond donor (HBD) such as glycerol, urea and carboxylic acid [17]. They exhibit desirable properties, like low volatility, non-flammability, biodegradability, affordability and ease of preparation [16, 18]. DES-based functionalization has been increasingly explored for nanomaterials to tailor surface chemistry and enhance adsorption performance in water and wastewater treatment applications [19]. Functionalizing MWCNTs with DESs can alter surface characteristics, improve dispersion and introduce active functional sites that enhance adsorption performance [20, 21]. Prior studies have shown that DES-modified CNTs are effective in removing heavy metals such as mercury [22] and lead [23], suggesting their potential in adsorbing organic contaminants as well. In addition to enhancing surface functionality, DES modified MWCNTs are expected to influence the adsorption mechanism of ibuprofen through multiple synergistic interactions. The aromatic ring of ibuprofen can engage in π–π stacking interactions with the graphitic surface of MWCNTs. This interaction contributes significantly to adsorption affinity. Further, hydrogen bonding interactions may form between the carboxyl group of ibuprofen and the hydroxyl groups of glycerol present in the DES coating. Electrostatic attraction also plays a crucial role, particularly under slightly acidic conditions, where partially deprotonated Ibuprofen molecules interact with the positively charged quaternary ammonium groups derived from tetrabutylammonium bromide.

Despite the extensive research on carbon nanotube-based adsorbents and the growing interest in DESs for material modification, clear gaps remain in the application of DES-functionalized nanomaterials for pharmaceutical wastewater treatment. Previous studies on DES-modified carbon nanotubes primarily focused on the removal of inorganic contaminants, particularly heavy metals, with limited attention given to organic pharmaceutical compounds. Moreover, existing investigations on ibuprofen removal using CNT-based adsorbents largely rely on conventional surface functionalization strategies or single-factor optimization approaches, without incorporating green solvent modification or advanced predictive modeling techniques.

In this context, the present study uses oxidized multi-walled carbon nanotubes (o-MWCTs) that were functionalized with a DES composed of tetrabutylammonium bromide (TBAB) as HBA and glycerol as HBD. The goal was to assess the efficiency of DES-functionalized MWCNTs in removing ibuprofen from pharmaceutical wastewater. The synthesized material was characterized, and adsorption experiments were performed under batch conditions at the specified parameters pH, temperature and contact time. The adsorption behaviour was interpreted through using Langmuir and Freundlich isotherm models, while kinetic studies were performed to identify the most suitable rate controlling model for the ibuprofen uptake process. Although DES-modified MWCNT's were reported for heavy metal adsorption, no previous work has explored TBAB-glycerol DES functionalization for the removal of ibuprofen or other pharmaceutical contaminants. To the best of our knowledge, this is the first report employing TBAB–glycerol DES for CNT functionalization

targeting pharmaceutical contaminants. In addition to material innovation, this work uniquely integrates artificial neural networks (ANNs) with response surface methodology (RSM) to achieve dual predictive optimization analysis of the adsorption process. This combined modeling approach enables accurate performance prediction, identification of complex nonlinear relationships among operating parameters, and systematic optimization within a single framework. The study therefore advances existing knowledge by coupling a green surface modification strategy with efficient data-driven modeling, addressing critical gaps in both material design and process optimization for pharmaceutical contaminant removal.

2 Materials and methods

2.1 Materials

Ferric nitrate nonahydrate (99.95% purity), aluminium nitrate nonahydrate (99% purity), gases including argon, hydrogen, and acetylene/ethylene, were purchased from Sri Sai Scientific Company (Coimbatore, Tamilnadu, India). Ibuprofen (reagent grade, 99% purity) was purchased from Alpha Chemika (Mumbai, Maharashtra, India). H_2SO_4 and HNO_3 (99% purity), ethanol I.P. (~99% purity), tetra-n-butyl ammonium bromide (TBAB, ≥99% purity), deionised water and anhydrous glycerol (≥99% purity) were obtained from Imperial Scientific Works (Coimbatore, Tamilnadu, India).

2.2 Preparation of multi-walled carbon nanotubes

2.2.1 Catalyst preparation

To promote CNT development, a Fe_2O_3/Al_2O_3 catalyst was created by coprecipitation. $Fe(NO_3)_3 \cdot 9H_2O$ and $Al(NO_3)_3 \cdot 9H_2O$ aqueous solutions were combined at 80 °C while being continuously stirred, and then they were dried for 12 h at 100 °C. To produce catalyst particles that were nanosized (15–20 nm), the dried precursor was pulverised, calcined at 650 °C for 6 h, and sieved. During CNT synthesis, the alumina support increased the catalytic activity, reduced agglomeration and encouraged dispersion.

2.2.2 Synthesis of multi-walled carbon nanotube

A horizontal split-tube quartz furnace was used as part of a thermal chemical vapour deposition system for the synthesis. The catalyst, weighing between 0.1 and 0.5 g, was positioned in the middle of the furnace. The quartz tube was gradually heated to the target temperature (600–1000 °C) at a rate of 15 °C/min after being purged with 250 cm^3/min STP (standard temperture and pressure) of argon. Acetylene/ethylene (100 cm^3/min STP) and hydrogen (100–250 cm^3/min STP) were added simultaneously after stabilisation. Depending on the run, growth was maintained for 30 to 60 min before the system was cooled to room temperature using argon flow.

2.2.3 Purification of multi-walled carbon nanotubes

The as-grown MWCNTs were purified through acid treatment to eliminate residual metal catalysts and amorphous carbon impurities. Approximately 1 g of MWCNT was dispersed in a mixed acid solution containing concentrated H_2SO_4 and HNO_3 (v/v 3:1) and subjected to ultrasonication at 40 °C for 3 h. This treatment not only eliminated contaminants, but also added oxygen-containing groups to the nanotube surface [12]. The suspension was diluted with 300 mL deionised water, filtered using a polytetrafluoroethylene (PTFE) membrane and washed till neutral. The oxidised MWCNT was dried at 70 °C for 6 h.

2.3 Preparation of deep eutectic solvent

The DES was prepared by combining TBAB (HBA) and glycerol (HBD) at a molar ratio of 1:4. TBAB (322.37 mg) and glycerol (368.36 mg) were combined in a beaker and stirred continuously at 80 °C until a clear, homogeneous, and stable liquid was formed.

2.4 Functionalization of oxidized multi-walled carbon nanotubeswith deep eutectic solvent

Oxidized MWCNT (o-MWCNT) (200 mg) were added to 7 mL of the prepared TBAB-glycerol DES. The resulting mixture was subjected to ultrasonication at 60 °C for 2 h to ensure complete dispersion and promote the interaction between the o-MWCNTs and the DES. After sonication, the mixture was filtered and washed thoroughly with ethanol to remove any unreacted DES. The obtained DES-functionalized MWCNT was subjected to drying at 80 °C in a hot air oven to ensure complete removal of the residual solvent.

2.5 Adsorption experiment

Adsorption studies were performed under batch conditions to assess the performance of DES-functionalized MWCNTs towards ibuprofen removal. A stock solution of ibuprofen (50 mg/L) was prepared in distilled water. For each experiment, a predetermined mass of adsorbent (0.03 g) was added to a fixed volume of ibuprofen solution (e.g., 40 mL) with a known initial concentration (C_0 = 50 mg/L) in a conical flask. The samples were placed on an orbital shaker at a constant speed of 100–120 rpm. The key parameters such as temperature (15–65 °C), contact time (30–180 min) and

pH (2–10) were investigated to find the optimum conditions for maximum ibuprofen removal.

After agitation for the specified time, the mixture was filtered and the residual ibuprofen content was determined with a double beam UV-Vis spectrophotometer (Labman Scientific Instruments, India) at λ_{max} = 264 nm. The amount of ibuprofen adsorbed Q (mg/g) was calculated using the following equations:

$$Q = (C_0 - C_i) \times \frac{V}{M}, \quad (1)$$

where V is the volume of the solution (L), C_0 (mg/L) is the initial concentration and C_i (mg/L) is the final concentration of ibuprofen and M is the mass of the adsorbent (g).

2.6 Adsorption kinetics

The kinetic studies were carried out by performing a time-dependent adsorption study under optimum conditions (temperature = 35 °C and pH = 4). The ibuprofen removal percentage was determined by fixing the initial concentration (C_0 = 50 mg/L) and varying the contact time from 0 to 150 min. The experimental data were analyzed using pseudo-first-order, pseudo-second-order, and intra-particle diffusion kinetic models.

2.7 Adsorption isotherm studies

Isotherm experiments were conducted by varying the initial ibuprofen concentration (50, 45, 35, 0, 25 and 20 mg/L) while keeping the adsorbent dosage (30 mg), volume (40 mL), temperature (35 °C), pH (4), and contact time (90 min) constant at their optimal values. The equilibrium data were fitted to the Langmuir and Freundlich isotherm models using linear regression.

2.8 Desorption studies

Desorption studies were conducted to evaluate the regeneration potential of ibuprofen loaded-MWCNTs. A known mass (30 mg) of ibuprofen-loaded MWCNT, obtained after adsorption equilibrium, was contacted with 30 mL of ethanol as the desorbing agent in hot plate magnetic stirrer. The experiment was conducted at 50 °C and the desorption process was investigated as a function of contact time (30–150 min). The desorption efficiency was calculated using the formula

$$\text{Desorption efficiency} = \frac{Q_d}{Q_e} \times 100 \quad (2)$$

where Q_d is amount desorbed (mg/g) and Q_e is equilibrium adsorption capacity

2.9 Artificial neural network

ANNs have been increasingly applied to describe complex and nonlinear adsorption systems. They provide a practical way to predict adsorption trends in cases were empirical or regression models shows limitation. With respect to ibuprofen removal from pharmaceutical waste water, ANN modelling helps in simulation adsorption performance by linking key operating factors such as temperature, contact time, pH and dosage [24].

2.10 Response surface methodology

Based on preliminary batch adsorption experiments, pH, contact time, and temperature were identified as key parameters influencing pollutant removal. Response surface methodology using a Box–Behnken design was employed to optimize these parameters [24].

2.11 Characterization techniques

The functional groups and chemical interactions were analyzed using Fourier Transform Infrared Spectroscopy (FTIR, Shimadzu IRTracer-100, Shimadzu Corporation, Japan) in the range of 4000–400 cm^{-1}. The surface morphology and structural characteristics of the samples were examined using Field Emission Scanning Electron Microscopy (FESEM, ZEISS SIGMA FESEM, Carl Zeiss AG, Germany). The results of the adsorption studies, kinetics, isotherms and desorption studies were identified using UV-Vis double beam spectrometer (Prolab UV 295 Advance UV-VIS Double Beam Spectrophtometer, Medsun Biomedical Technologies Pvt Ltd, Delhi, India). All measurements were conducted under standard operating conditions as specified by the instrument manufacturers.

3 Results and discussion

3.1 Deep eutectic solvent characterization

3.1.1 Fourier transform infrared analysis

The presence of both components and their interaction were confirmed by the FTIR spectrum's distinctive peaks (Fig.1). Due to substantial hydrogen bonding inside the DES structure, the O−H stretching vibrations of the hydroxyl groups in glycerol are responsible for the wide absorption band seen at around 3356 cm^{-1} [20, 25]. The asymmetric and symmetric C−H stretching vibrations of the alkyl chains in TBAB and glycerol are represented by peaks at 2965 cm^{-1} and 2876 cm^{-1}. The peaks at 1652 cm^{-1} and 1108 cm^{-1} that may be connected to C-N vibrations or ammonium group functions further suggest the existence of TBAB [20]. The methyl groups ($-CH_3$)

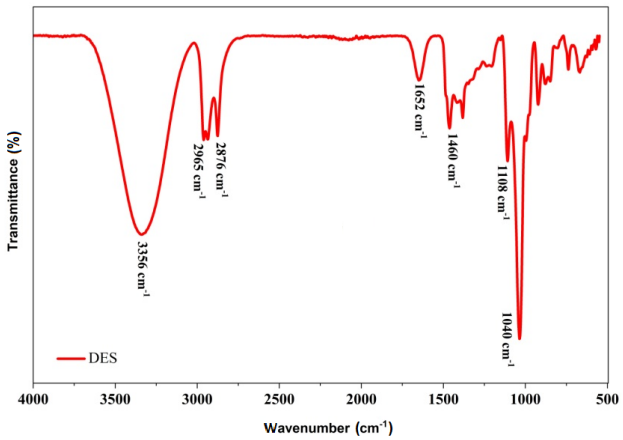

Fig. 1 FTIR spectrum of the DES

showed bending vibrations at 1460 cm^{-1} and 1382 cm^{-1}. The overall spectrum is consistent with the formation of a hydrogen-bonded network between the quaternary ammonium salt (TBAB) and the hydrogen bond donor (glycerol), confirming the successful synthesis of the DES.

3.2 Adsorbent characterization

3.2.1 Fourier transform infrared analysis

From the Fig. 2 the asymmetric stretching vibrations of C–N and potential interactions from TBAB-related quaternary ammonium functional groups are indicated by a large and sharp absorption band at around 2340–2276 cm^{-1}. Furthermore, hydrogen-bonded systems resembling glycerol-based DES are shown in the peaks at 2041–2002 cm^{-1}. The alteration of the bromide-containing tetra-n-butylammonium cation on the MWCNT surface is confirmed by the low wavenumber band at 670 cm^{-1}, which shows C–Br stretching vibrations. This finding is consistent with other observations in the literature that emphasise C–Br bands in the 550–700 cm^{-1} area as a sign of the presence of TBAB-based DES [26]. The current FTIR does not show the characteristic O–H stretching (~3400 cm^{-1}) or C=O stretching that is frequently seen in pristine or oxidised MWCNTs. This implies that following DES functionalisation, carboxylic or hydroxyl groups are reduced. Similar results with DES-functionalized MWCNT's reduced O–H and C=O peaks are also reported in [26]. These changes improve the affinity of Ibuprofen adsorption onto the surface of MWCNTs and provide novel adsorption sites.

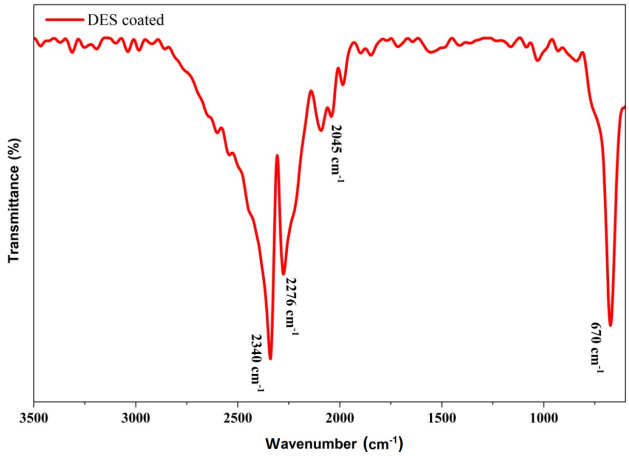

Fig. 2 FTIR spectrum of the DES coated MWCNT

3.2.2 Field emission scanning electron microscopy analysis

The field emission scanning electron microscopy (FESEM) (ZEISS SIGMA FESEM, FEI/Thermo Fisher Scientific, USA) images (Fig. 3) revealed that the functionalization process altered the surface morphology of

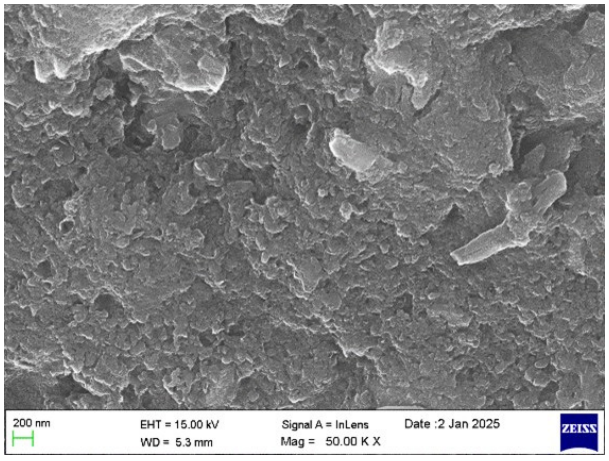

(a)

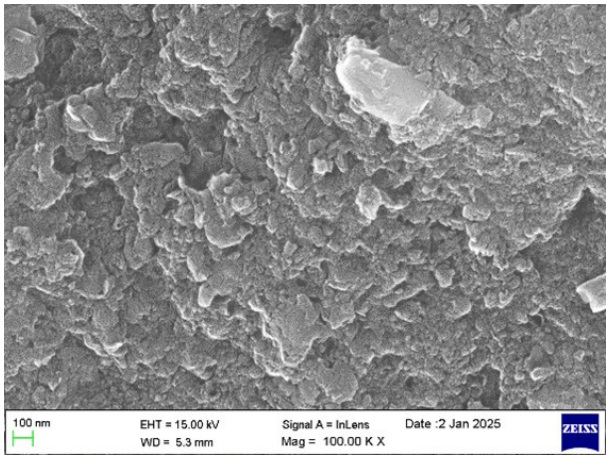

(b)

Fig. 3 FESEM images of DES functionalized MWCNTs: (a) scale bar = 200 nm and (b) scale bar = 100 nm

the MWCNTs. Compared to pristine MWCNTs (which typically appear as smoother, entangled tubes), the DES modified MWCNTs (DES-MWCNTs) exhibited a rougher surface texture. This roughness suggests the coating or attachment of the DES onto the nanotube surfaces. Some degree of aggregation or bundling of the nanotubes was observed. The morphological alterations, especially the increased surface roughness, suggest the formation of possibly more active adsorption sites.

3.3 Adsorption studies

The *Removal* % of ibuprofen was determined using the following equation

$$Removal\ \% = \frac{C_0 - C_i}{C_0} \times 100\,, \tag{3}$$

where C_0 and C_i denotes initial and final concentration, respectively, in mg/L. Temperature (15 °C to 55 °C) and contact time (30 to 180 min) were investigated to determine the best conditions for greatest removal rate.

3.3.1 Effect of temperature

From Fig. 4 it can be observed that the removal efficiency increased from 39.66% at 15 °C to a maximum of 94.98% at 35 °C. Beyond this temperature, efficiency remains almost constant up to 65 °C. The initial rise in temperature enhances the thermal motion of ibuprofen molecules, improving their diffusion towards the adsorbent surface and facilitating interaction with the active sites. Once the temperature exceeds 35 °C, the adsorption sites are approaching saturation, resulting in no noticeable increase in removal efficiency.

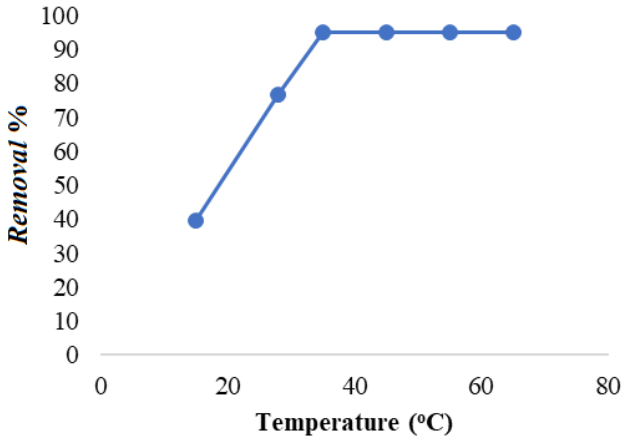

Fig. 4 Effect of temperature on *Removal* % (at contact time = 90 min and pH=4)

3.3.2 Effect of contact time

It is evident that the adsorption shows a quick rise in removal efficiency, attaining about 40.26% within the first 30 min and reaching nearly 94.9% after 90 min (Fig. 5). The gradual increase observed at the beginning is mainly due to the increased availability of active binding sites on the adsorbent surface, allowing ibuprofen molecules to diffuse rapidly and attach more easily. When the contact time exceeded 90 min, only a slight removal change was noted, which states that system reached its equilibrium stage. By this stage, most of the adsorbent sites have been filled, while few remaining ones become harder for ibuprofen molecules to reach because of steric hindrance and electrostatic repulsion. Thus, a contact time of 90 min was determined to be optimal for achieving the highest ibuprofen removal efficiency.

3.3.3 Effect of pH

From the Fig. 6 it can be concluded that under strongly acidic conditions (pH 2), the removal efficiency was fairly

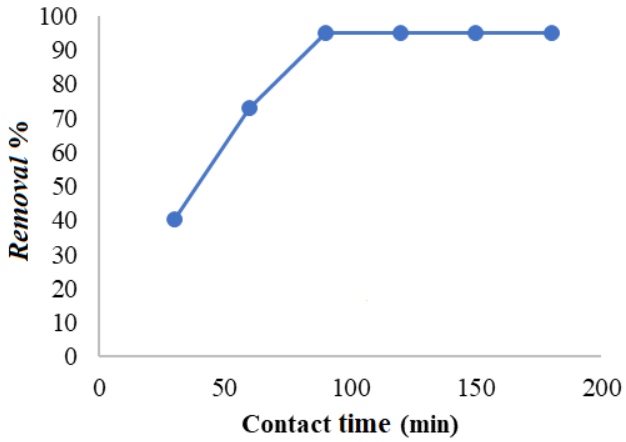

Fig. 5 Effect of contact time on *Removal* % (temperature = 35 °C and pH = 4)

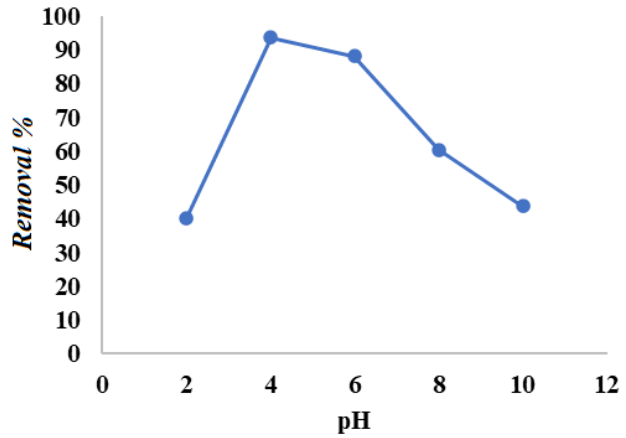

Fig. 6 Effect of pH on *Removal* % (at contact time = 90 min and temperature = 35 °C)

low (around 40%) because ibuprofen mainly remains in neutral form, while the protonated adsorbent surface offers only limited electrostatic attraction. When the pH neared the p*K*a of ibuprofen (~4.91,[16]), the adsorption efficiency rose gradually and reached its maximum value of about 93% at pH 4. The optimum performance can be attributed to several favorable interactions such as electrostatic attractions between partially deprotonated ibuprofen molecules and the positively charged quaternary ammonium sites of the DES, hydrogen bonding through hydroxyl groups of glycerol, and π–π interactions between the aromatic rings of ibuprofen and MWCNT surface [27]. Even at pH 6, adsorption efficiency remains relatively high (around 88%), however it dropped noticeably as the solution becomes more alkaline- approximately 60% at pH 8 and 44% at pH 10. At higher pH levels, the adsorbent surface acquires a negative charge, resulting in electrostatic repulsion between the surface and ibuprofen anions, which consequently reduces adsorption efficiency.

3.4 Adsorption kinetics

3.4.1 Pseudo first order kinetics

From Fig. 7, the linear plot of log (Q_e–Q_t); where Q_t is adsorption capacity at contact timet) against time produced a correlation coefficient of (R^2 = 0.8406), showing that model provided only a moderate level of fit. From the slope and intercept of regression line, the first order rate constant K_1 = 0.0087 min^{-1} and the calculated equilibrium adsorption capacity Q_e(cal) = 59.29 mg/g were obtained. However, this calculated value was lower than the experimental measured Q_e(exp) = 86.2 mg/g, implying that the model tends to underestimate the true adsorption capacity (Table 1) [25]. The difference suggests that the adsorption of ibuprofen onto MWCNT is influenced by more than just simple physisorption through boundary layer diffusion. It likely includes stronger forces such as electrostatic attraction, hydrogen bonding and π–π interactions between the adsorbent and adsorbate molecules.

3.4.2 Pseudo second order kinetics

The linear plot of t/Q_t vs time yielded a high correlation coefficient of R^2 = 0.9715, indicating that the pseudo second order kinetic model accurately describes the adsorption process. This close agreement implies that chemisorption plays a major role in determining the overall adsorption rate. The equilibrium adsorption capacity Q_e(cal) = 86.96 mg/g estimated from the model was consistent with the experimentally observed value Q_e(exp) = 86.2 mg/g (Fig. 8) confirming the model's reliability and the strong affinity of

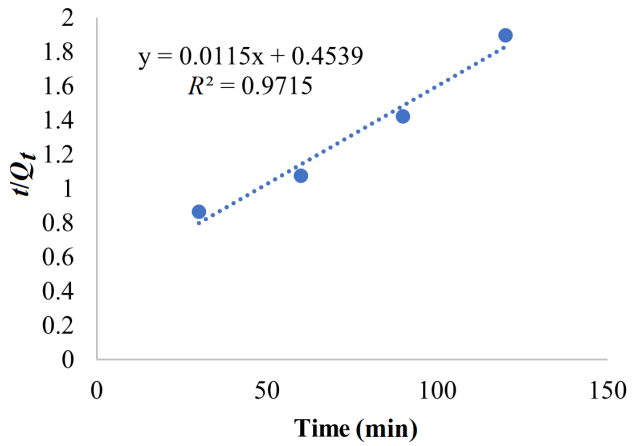

Fig. 7 Pseudo first order kinetics

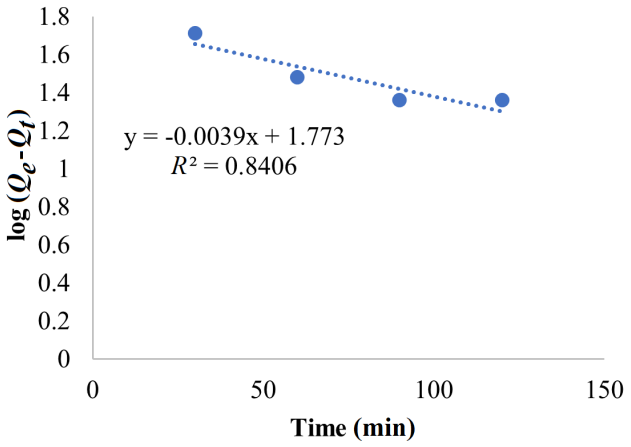

Fig. 8 Pseudo second order kinetics

Table 1 Parameters for kinetic models diffusion

Pseudo first order [25]				Pseudo second order [28]				Intra-particle diffusion model [29]		
$\log(Q_e - Q_t) = \log Q_e - \left(\frac{K_1}{2.303}\right)t$				$\frac{t}{Q_t} = \frac{t}{Q_e} + \frac{1}{K_2 Q_e^2}$				$Q_t = K_{id}t^{0.5} + C$		
Q_e exp (mg/g)	Q_e (cal) (mg/g)	K_1 (1/min)	R^2 (first order)	Q_e (exp) (mg/g)	Q_e (cal) (mg/g)	K_2 (g/mg·min)	R^2	K_{id} (mg/g · min 0.5)	R^2	C (mg/g)
86.2	59.29	0.008751	0.8406	86.2	86.96	0.000291	0.9715	5.3367	0.867	9.3522

DES-MWCNTs to ibuprofen under the optimized conditions (Table 1) [28]. The calculated second order rate constant K_2 = 0.000291 g/mg · min further supports the efficient adsorption behavior of the system within the studied range.

3.4.3 Intra-particle diffusion model

From Fig. 9, a plot of adsorbed capacity (Q_t) *versus* the square root of time ($t^{0.5}$) produced a linear trend with an R^2 = 0.867, indicating that intra-particle diffusion plays a significant role in the adsorption process, though it is not the only rate-controlling mechanism. The slope of the line (K_{id} = 5.3367) corresponds to the intra-particle diffusion rate constant (K_{id}), whereas the intercept (C = 9.3522, where C refers to boundary layer thickness constant) reflects the influence of the boundary layer surrounding the adsorbent particles (Table 1) [29]. The positive intercept implies both surface adsorption and intra-particle diffusion are operative throughout the adsorption, rather than diffusion being the exclusive limiting factor.

3.5 Adsorption isotherm

At constant temperature, the relationship between the equilibrium concentration of the solute in solution and the quantity adsorbed on the adsorbent surface is expressed through adsorption isotherms. To comprehend the adsorption mechanism, the experimental data collected at 35 °C, 90 min and pH 4 were fitted to the linear forms of the Langmuir and Freundlich models.

The Langmuir isotherm assumes monolayer adsorption onto a homogeneous surface with a finite number of identical adsorption sites and no interaction between adsorbed molecules [30, 31]. A plot of $1/C_e$ *versus* $1/C_e$ (Fig. 10) yielded a straight line, and the values of maximum adsorption capacity Q_{max} and Langmuir constant K_L were determined from the slope and intercept of this plot, respectively. The Q_{max} was 86.20 mg/g, with a K_L of 0.5156 L/mg (Table 2) [30]. The correlation coefficient R^2 = 0.9602 suggests that the Langmuir model accurately represents the experimental data.

The Freundlich isotherm is an empirical model that explains multilayer adsorption occurring on a heterogeneous surface where adsorption sites are unevenly distributed and interactions exists among the adsorbed molecules [11]. When ln Q_e is plotted against ln Q_e (Fig. 11), a clear linear relationship is observed. The Freundlich constant K_F and n were derived from the intercept and slope of the corresponding linear plot. The calculated value of K_F was 4.42 (mg/g)(L/mg)$^{(1/n)}$ (in Table 2) [31], while n was determined to be 2.3186. The Freundlich model exhibited a correlation coefficient (R^2 = 0.9397), indicating good agreement between the experimentally observed adsorption data and the values predicted by the model.

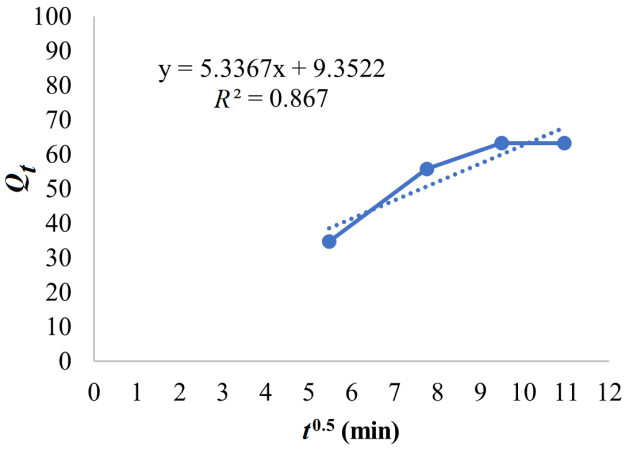

Fig. 9 Intra-particle diffusion model

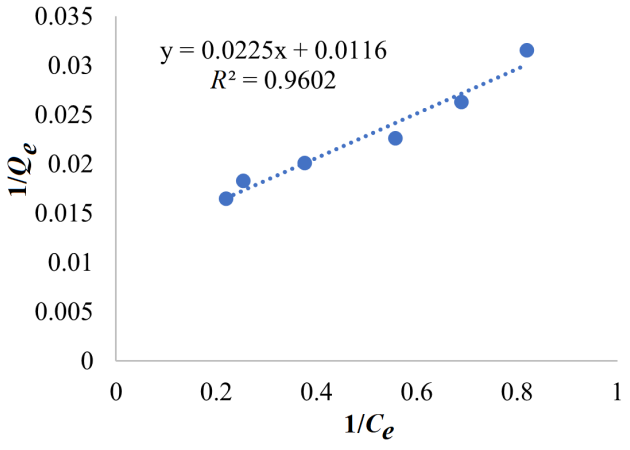

Fig. 10 Linear Langmuir plot

Table 2 Adsorption isotherm parameters

Isotherm model	Linear model expression	R^2	Q_{max} (mg/g)	K_L (L/mg)
Langmuir	$\frac{1}{Q_e} = \frac{1}{Q_{max} K_L} \frac{1}{C_e} + \frac{1}{Q_{max}}$	0.9602	86.20	0.5156
		R^2	n (–)	K_F (mg/g) (L/mg)$^{(1/n)}$
Freundlich	$\ln Q_e = \ln K_F + \frac{1}{n} \ln C_e$	0.9397	2.3186	4.4817

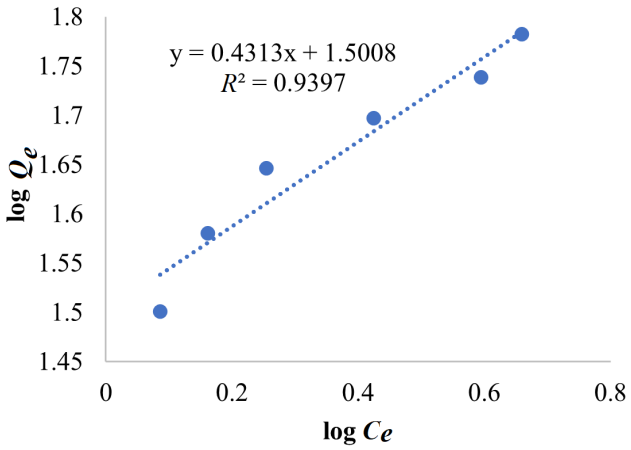

Fig. 11 Linear Freundlich plot

A comparison of the regression coefficients revealed that the Langmuir model (R^2 = 0.9602) provided a marginally better representation of the experimental data than the Freundlich model (R^2 = 0.9397). This suggests that the adsorption of ibuprofen onto DES-MWCNTs might involve a heterogeneous surface and potentially multilayer adsorption. The value of $n > 1$ (2.32) from the Freundlich isotherm indicates a favourable adsorption process.

3.6 Desorption studies

The amount of ibuprofen desorbed increased steadily from 20.12 mg/g at 30 min to 83.20 mg/g after 180 min, indicating effective release of the adsorbed ibuprofen molecules into the solvent. For this study, the equilibrium adsorption capacity of Q_e = 86.2 mg/g was considered (from Langmuir isotherm model), it was observed that a desorption efficiency exceeding 96% was achieved at equilibrium (Fig. 12). The high desorption efficiency suggests that the adsorption of ibuprofen onto DES-MWCNTs is predominantly governed by reversible interactions, including π–π stacking, hydrogen bonding, and electrostatic attraction.

The desorption study adequately demonstrates the reusability of the DES-modified MWCNTs within the scope of the present work.

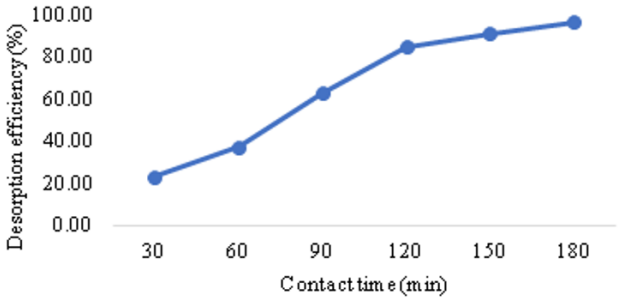

Fig. 12 Contact time vs desorption efficiency

3.7 Artificial neural network studies

In this work, an artificial neural network model was constructed and optimized to forecast the ibuprofen removal efficiency under varying experimental parameters (Fig. 13). The network architecture and learning algorithm were optimized to achieve a minimal mean squared error (MSE) 0.19 and a high coefficient of determination (R^2 = 0.998) (Table 3). The results predicted by ANN closely matched experimental observations, effectively capturing thermodynamic, kinetics and equilibrium trends.

3.7.1 Effect of temperature

From Fig. 14 it can be observed that the removal efficiency increased significantly from 39.66% at 15 °C to a maximum of 94.9% at 35 °C, indicating enhanced molecular

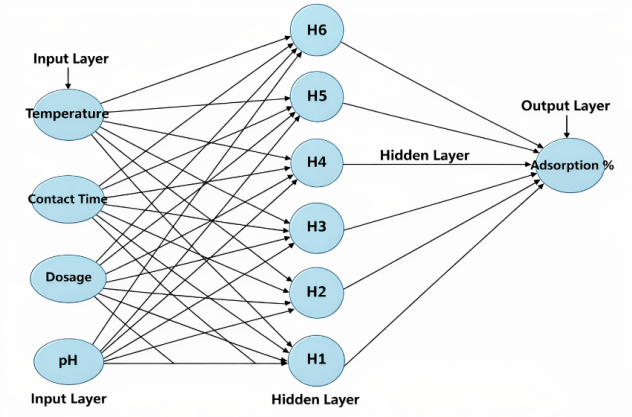

Fig. 13 ANN architecture for the adsorption of DES coated MWCNTs

Table 3 Minimal mean squared error and R^2 with its observation for DES coated MWCNT

Parameter	MSE	R^2	Observation
Dosage (g)	0.49	0.998	Removal increased from 73.4% to 94.9% with increasing dosage due to additional active sites. ANN demonstrated strong generalization for dosage variations.
Temperature (°C)	0.34	0.999	Removal increased from 39.66% to 94.9% up to 35 °C then remained constant at higher temperature.
Contact time (min)	0.19	0.999	Rapid uptake until 90 min (94.9% removal) reaching equilibrium. Lowest MSE shows high kinetic prediction accuracy.
pH	0.36	0.998	Maximum removal (94.9%) at pH 4. Lower adsorption at extreme pH values due to surface charge and ibuprofen ionization effects. ANN effectively modeled this non-linear behavior

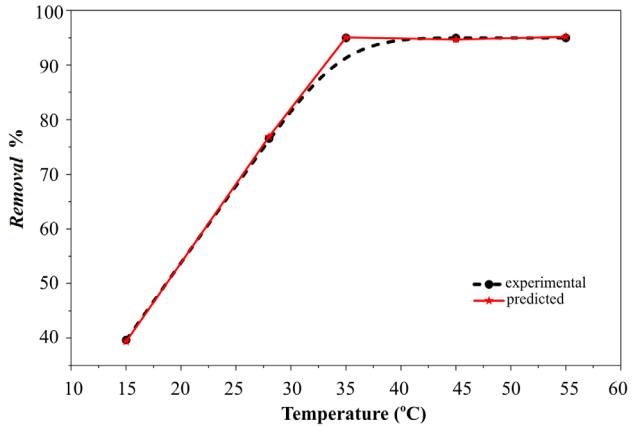

Fig. 14 Effect of temperature with its experimental and predicted values

mobility and improved interaction between ibuprofen and the DES-coated MWCNTs surface at moderate temperature. At temperatures above 45 °C, there is no significant change in the Removal %. The ANN predictions closely represented this experimental trend with minimal deviation, demonstrating the model's strength in accurately capturing the temperature-dependent adsorption behavior.

3.7.2 Effect of pH

The effect of pH on ibuprofen adsorption was examined between pH 2–10. Both experimental results and ANN-predicted values revealed that the maximum removal efficiency of 94.9% occurred at pH 4 (Fig. 15). Deviations from this pH resulted in reduced adsorption, which is attributed to changes in the surface charge of the adsorbent and the ionization state of ibuprofen. At highly acidic or basic conditions, the electrostatic interaction between the adsorbent and ibuprofen becomes less favorable, reducing uptake. The strong agreement between experimental and ANN outputs confirms the ability of the ANN model to capture the complex, nonlinear influence of pH on adsorption performance.

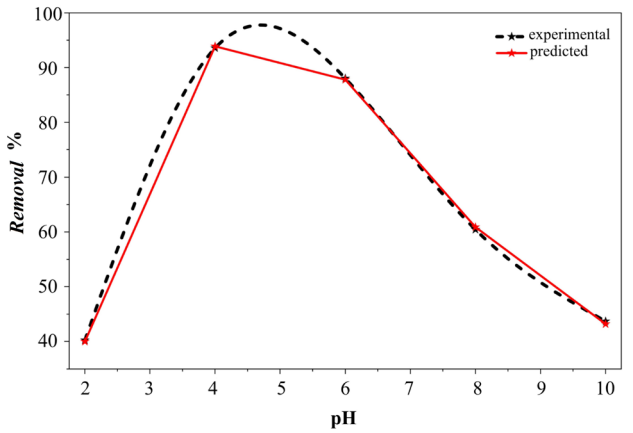

Fig. 15 Effect of pH with its experimental and predicted values

3.7.3 Effect of contact time

In Fig. 16 the effect of contact time on ibuprofen adsorption was studied within the range of 30 to 180 min. The removal efficiency rose quickly from 40.26% at 30 min to 94.9% at 90 min, showing that most adsorption occurred during the initial phase. After 90 min the rate of adsorption approached equilibrium, reaching 94.92% at 120 min and 94.99% at 180 min. The ANN prediction follows the same trend as the experimental results, demonstrating that the model effectively describes the adsorption kinetics and accurately reflects the observed behavior.

3.7.4 Effect of dosage

Fig. 17 shows the effect of Removal % for different adsorbent dosage (10–40 mg) by keeping all other parameters constant (i.e., at 35 °C, pH 4 and 90 mins). The removal efficiency increased progressively from 73.4% (10 mg) to 94.9% (40 mg), primarily due to the higher availability of active adsorption sites with increasing dosage. The ANN predictions were in strong agreement with experimental outcomes, demonstrating the model's capability to represent the influence of adsorbent dosage on adsorption efficiency.

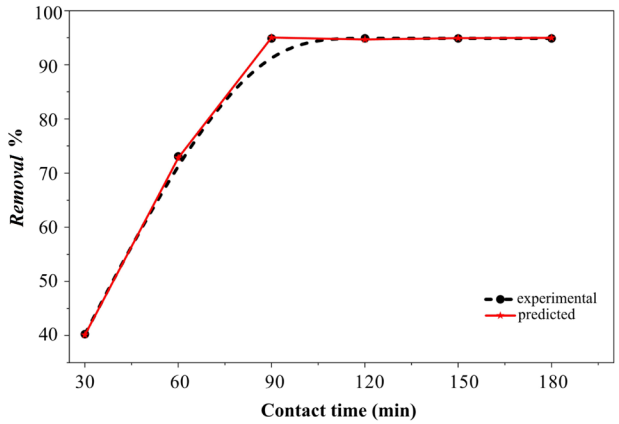

Fig. 16 Effect of contact time with its experimental and predicted values

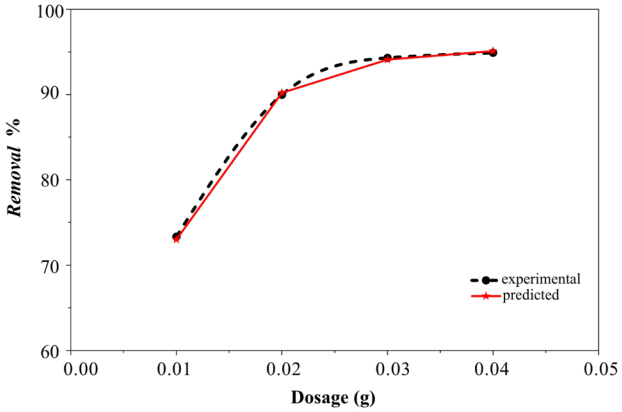

Fig. 17 Effect of dosage with its experimental and predicted values

It is also confirmed that the back propagation-trained ANN serves as a dependable computational approach for simulating ibuprofen adsorption across different operating conditions.

3.8 Response surface methodology

The optimization of pollutant removal efficiency was performed using the RSM based on Box-Behnken design. Three operating parameters pH (*A*), contact time (*B*) and temperature (*C*) were considered as independent variables, while the removal efficiency served as response factor. A total of 13 experimental runs were conducted to assess both the individual and interactive influences of these parameters on the overall pollutant removal.

3.8.1 Experimental design

The design matrix and corresponding pollutant removal efficiencies are shown in Table 4. Experimental results revealed that the pollutant removal percentage varies from 84.34% to 94.9% at different operating conditions. The maximum removal efficiency was achieved at pH 4, contact time 90 min and temperature 35 °C. The statistical significance of each parameter and their interactions was achieved through analysis of variance (ANOVA).

3.8.2 Statistical modeling and ANOVA

ANOVA results demonstrated that pH (F = 1922.44, p = 0.000026) was the most influential factor affecting pollutant removal followed by contact time (F = 161.64, p = 0.00105) and temperature (F = 16.38, p = 0.027). The F-value represents the ratio of variance explained by the model to the residual variance, indicating the relative significance of each factor, while the p-value indicates the probability that the observed effect is due to random error, with values less than 0.05 considered statistically significant. The interactions effects (*AB*, *AC* and *BC*) were also significant ($p < 0.05$), showing that the combined influence of parameters plays a crucial role in determining the removal performance. Here, *A*, *B*, and *C* correspond to pH, contact time, and temperature, respectively, while *AB*, *AC*, and *BC* represent their pairwise interaction effects. The quadratic terms (A^2, B^2 and C^2) exhibiting strong significance, confirming a curved response surface and justifying the use of second order model. The quadratic polynomial model was expressed as:

$$Y = 91.89 - 3.03A + 0.89B + 0.27C - 0.50AB + 0.25AC - 0.20BC - 1.12A^2 - 0.83B^2 - 0.55C^2 \quad (4)$$

where Y denotes the predicted removal efficiency.

The model exhibited an excellent correlation between exhibited and predicted results, with high coefficient of determination (R^2 = 0.9989) and adjusted (R^2 = 0.9955), confirming the accuracy and adequacy of the model.

Model summary: R^2 = 0.9989; Adjusted R^2 = 0.9955

The adjusted R^2 accounts for the number of predictors in the model and provides a more reliable measure of model fit. Table 5 presents the ANOVA results for the quadratic model, where the sum of squares quantifies the contribution of each factor to the total variation in the response, and the residual represents the unexplained variation between experimental and predicted values. The ANOVA results indicate that the developed RSM model demonstrates statistical relevance, as shown by a high F-value and p-values below 0.05 for the main factors. Here, Df represents the degrees of freedom associated with each model term, indicating the number of independent effects used in the ANOVA analysis. The reliability and predictive capabilities of the model is confirmed

Table 4 Experimental design matrix and observed responses

Run	pH	Time (min)	Temperature (°C)	*Removal* %
1.0	6.0	30.0	30.0	88.16
2.0	4.0	120.0	30.0	90.54
3.0	6.0	30.0	45.0	88.12
4.0	6.0	120.0	45.0	89.07
5.0	2.0	75.0	30.0	91.78
6.0	10.0	75.0	30.0	84.96
7.0	4.0	75.0	45.0	90.55
8.0	10.0	75.0	45.0	85.46
9.0	2.0	30.0	37.5	88.73
10.0	10.0	30.0	37.5	84.34
11.0	4.0	90	35	94.99
12.0	10.0	120.0	37.5	84.41
13.0	4.0	75.0	37.5	91.94

Table 5 ANOVA results for the quadratic model

Source	Sum of squares	Df	*F*-value	*p*-value
A (pH)	73.45	1	1922.44	2.6e-05
B (time)	6.18	1	161.64	0.00105
C (temperature)	0.63	1	16.38	0.027
AB	3.19	1	83.42	0.0028
AC	0.74	1	19.31	0.0218
BC	0.51	1	13.34	0.0354
A^2	15.86	1	415.05	0.00026
B^2	7.79	1	203.94	0.00074
C^2	2.86	1	74.82	0.00325
Residual	0.115	3	-	-

by the closeness of predicted and experimental values along with high R^2 and adjusted R^2 values. The statistically significant interaction between pH and contact time suggests that the adsorption performance is strongly governed by surface charge behaviour and mass transfer dynamics, which directly influence the accessibility of active adsorption sites.

The response surface and counter plots (Figs. 18 and 19) further showed that maximum pollutant removal occurs under slightly acidic conditions, moderate temperature and sufficient contact time.

3.8.3 Optimization

Numerical optimization predicted the optimal conditions for maximum pollutant removal as: pH = 4, time = 90 min., and temperature: 35 °C, yielding a predicted removal of 94.9%.

3.8.4 Experimental validation of the developed model

To validate the RSM model, additional experiments were carried out the experimentally determined best conditions (pH 4, time 90 min, temperature 35 °C). The model predicted a removal efficiency of 94.9% under these conditions, and the experimental measured removal were also found to be 94.9%, confirming excellent agreement between model and actual performance.

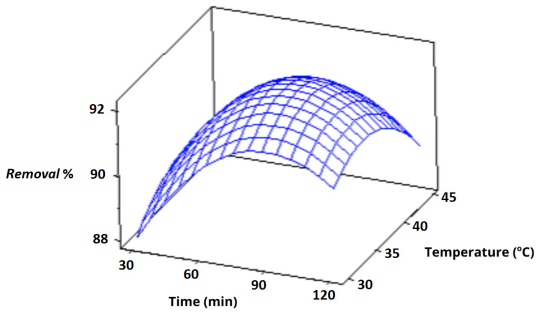

(a)

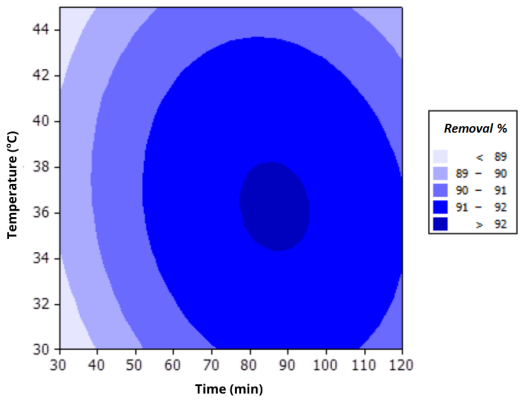

(b)

Fig. 18 Response surface plot showing interaction of temperature (a) and time (b) on *Removal* %

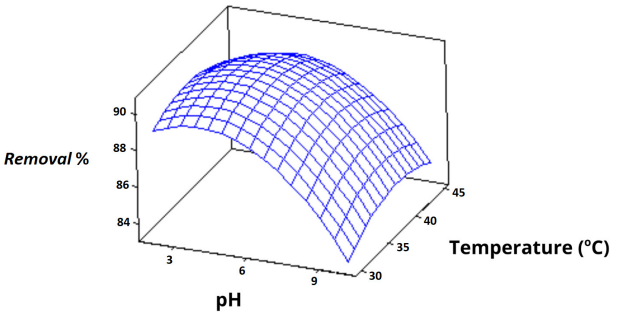

(a)

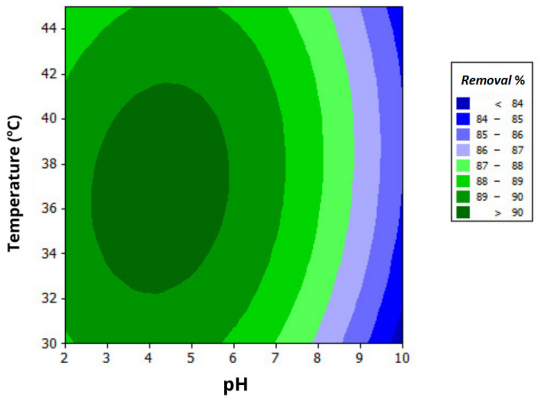

(b)

Fig. 19 3D response surface plot showing the interaction of pH (a) and temperature (b) on *Removal* %

3.8.5 Comparative discussion of sesponse surface methodology and artificial neural network models

Both RSM and ANN models effectively described and predicted the adsorption behavior of ibuprofen across in range of operational parameters. The RSM model, developed using the Box-Behnken experimental design, showed strong statistical reliability, achieving a coefficient of determination (R^2 = 0.9989) and an adjusted R^2 of 0.9955. In comparison, the ANN model displayed outstanding predictive accuracy, characterized very low minimal prediction error (MSE < 0.5) and consistently high correlation coefficients (R^2 > 0.998) across all parameters. Among tested architectures, the back propagation neural network containing ten hidden neurons and employing a ReLU activation function produced the most accurate prediction (MSE = 0.36, R^2 = 0.998). Unlike the RSM approach, which is limited by its predefined quadratic equation, the ANN model could flexibly learn and capture the non linear relationships among the pH, temperature, contact time and adsorbent dosage. Both the model performed well in predicting ibuprofen removal; however, the ANN provide marginally higher accuracy and better adaptability, particular under extreme parameter settings where non-linear effects were more prominent. Even so, the RSM model remains valuable because it offers clearer interpretability

and allows a detailed understanding of parameter interactions through ANOVA based statistical analysis.

4 Conclusion

The present investigation focuses on the synthesis and application of DES coated MWCNTs for ibuprofen removal from aqueous solutions. Deep eutectic solvents prepared from tetrabutylammonium bromide and glycerol effectively functionalized the oxidized MWCNT surface. FTIR spectra confirmed this modification through characteristic peaks at 2340–2276 cm^{-1} (C≡N stretch) and 670 cm^{-1} (C–Br stretch), validating successful surface functionalization. FESEM imaging also revealed an increase in surface roughness, which indicates the formation of additional active sites favorable for adsorption.

Batch experiments showed that the optimum operating conditions as 35 °C, pH 4, and 90-min contact time, under which a maximum removal efficiency reached 94.9%. The adsorption kinetics followed the pseudo second order model (R^2 = 0.9715) with the calculated adsorption capacity (Q_e(cal) = 86.96 mg/g) closely matching the experimental values (Q_e(exp) = 86.2 mg/g), suggesting chemisorption's as primary mechanism. The equilibrium adsorption data fitted well to the Langmuir isotherm model (R^2 = 0.9602, Q_{max} = 86.20 mg/g, K_L = 0.5156 L/mg), indicating monolayer adsorption on a homogeneous surface, the Freundlich model (R^2 = 0.9397), characterized by the constants and , showed favorable multilayer adsorption on heterogeneous sites, with an value of 2.3186, indicating favorable adsorption intensity.

Desorption studies further confirmed the regeneration capability of the DES functionalized MWCNTs. A desorption efficiency exceeding 96% relative to the equilibrium adsorption capacity was achieved, indicating effective recovery of ibuprofen from the adsorbent surface. The high desorption efficiency suggests that the adsorption process is predominantly governed by reversible interactions, supporting the reusability of the adsorbent and enhancing its suitability for sustainable and cost-effective wastewater treatment application.

The ANN model produced an MSE = 0.36 and R^2 = 0.998, accurately reproducing the experimental data across temperature, pH, contact time and dosage. Optimization using RSM supported these findings, yielding a high concentration (R^2 = 0.9989) and predicting the same optimal condition of pH 4, 90 min, and 35 °C with a removal efficiency of 94.9%. The prediction outcomes were in close agreement with the experimentally validated removal efficiency of 94.9% under identical condition. Taken together, these results indicate that DES functionalized MWCNTs behave as stable, reusable and ecofriendly adsorbent. The approach also demonstrates strong predictive reliability and shows clear potential for scale-up in practical wastewater- treatment applications.

Acknowledgements

We acknowledge the kind support of all laboratory staff who assisted during the experimental work.

References

[1] Chopra, S., Kumar, D. "Ibuprofen as an emerging organic contaminant in environment, distribution and remediation", Heliyon, 6(6), e04087, 2020. https://doi.org/10.1016/j.heliyon.2020.e04087

[2] National Center for Biotechnology Information "PubChem Compound Summary: Ibuprofen", [online] Available at: https://pubchem.ncbi.nlm.nih.gov/compound/Ibuprofen [Accessed: 14 September 2025]

[3] Jan-Roblero, J., Cruz-Maya, J. A. "Ibuprofen: toxicology and biodegradation of an emerging contaminant", Molecules, 28(5), 2097, 2023. https://doi.org/10.3390/molecules28052097

[4] Rivera-Utrilla, J., Sánchez-Polo, M., Ferro-García, M. Á., Prados-Joya, G., Ocampo-Pérez, R. "Pharmaceuticals as emerging contaminants and their removal from water. A review", Chemosphere, 93(7), pp. 1268–1287, 2013. https://doi.org/10.1016/j.chemosphere.2013.07.059

[5] Deb, C., Thawani, B., Menon, S., Gore, V., Chellappan, V., Ranjan, S., Ganesapillai, M. "Design and analysis for the removal of active pharmaceutical residues from synthetic wastewater stream", Environmental Science and Pollution Research, 26(18), pp. 18739–18751, 2019. https://doi.org/10.1007/s11356-019-05070-9

[6] Gonzalez-Rey, M., Bebianno, M. J. "Does non-steroidal anti-inflammatory (NSAID) Ibuprofen induce antioxidant stress and endocrine disruption in mussel Mytilus galloprovincialis?", Environmental Toxicology and Pharmacology, 33(2), pp. 361–371, 2012. https://doi.org/10.1016/j.etap.2011.12.017

[7] Zhang, X., Gao, C., Wang, R., Han, R. "Remediation of ibuprofen and naproxen in water by a green composite material of magnetic carbon nanotube–metal–organic framework", Journal of Environmental Chemical Engineering, 11(5), 111090, 2023. https://doi.org/10.1016/j.jece.2023.111090

[8] Dolatabadi, M., Ghorbanian, A., Ahmadzadeh S. "Mg–Al layered double hydroxide as promising sustainable nanoadsorbent for application in water/wastewater treatment processes; diethyl phthalate removal", Journal of Environmental Health and Sustainable Development, 6(3), pp. 1367–1375, 2021. https://doi.org/10.18502/jehsd.v6i3.7244

[9] Wang, Z., Srivastava, V., Ambat, I., Safaei, Z., Sillanpää, M. "Degradation of ibuprofen by UV-LED/catalytic advanced oxidation process", Journal of Water Process Engineering, 31, 100808, 2019. https://doi.org/10.1016/j.jwpe.2019.100808

[10] Ren, Z., Romar, H., Varila, T., Xu, X., Wang, Z., Sillanpää, M., Leiviskä, T. "Ibuprofen degradation using a Co-doped carbon matrix derived from peat as a peroxymonosulphate activator", Environmental Research, 193, 110564, 2021. https://doi.org/10.1016/j.envres.2020.110564

[11] Candido, J. P., Andrade, S. J., Fonseca, A. L., Silva, F. S., Silva, M. R. A., Kondo, M. M. "Ibuprofen removal by heterogeneous photocatalysis and ecotoxicological evaluation of the treated solutions", Environmental Science and Pollution Research, 23(19), pp. 19911–19920, 2016. https://doi.org/10.1007/s11356-016-6947-z

[12] Ayawei, N., Ebelegi, A. N., Wankasi, D. "Modelling and interpretation of adsorption isotherms", Journal of Chemistry, 2017(1), 3039817, 2017. https://doi.org/10.1155/2017/3039817.

[13] Smith, S. C., Rodrigues, D. F. "Carbon-based nanomaterials for removal of chemical and biological contaminants from water: A review of mechanisms and applications", Carbon, 91, pp. 122–143, 2015. https://doi.org/10.1016/j.carbon.2015.04.043

[14] Nabatian, E., Dolatabadi, M., Ahmadzadeh, S. "Application of experimental design methodology to optimize acetaminophen removal from aqueous environment by magnetic chitosan@multi-walled carbon nanotube composite: Isotherm, kinetic, and regeneration studies", Analytical Methods in Environmental Chemistry Journal, 5(1), pp. 61–74, 2022. https://doi.org/10.24200/amecj.v5.i01.168

[15] Nasrollahzadeh, M., Sajjadi, M., Iravani, S., Varma, R. S. "Carbon-based sustainable nanomaterials for water treatment: State-of-the-art and future perspectives", Chemosphere, 263, 128005, 2021. https://doi.org/10.1016/j.chemosphere.2020.128005

[16] Hanbali, G., Jodeh, S., Hamed, O., Bol, R., Khalaf, B., Qdemat, A., Samhan, S. "Enhanced ibuprofen adsorption and desorption on synthesized functionalized magnetic multiwall carbon nanotubes from aqueous solution", Materials, 13(15), 3329, 2020. https://doi.org/10.3390/ma13153329

[17] El Achkar, T., Greige-Gerges, H., Fourmentin, S. "Basics and properties of deep eutectic solvents: A review", Environmental Chemistry Letters, 19, pp. 3397–3408, 2021. https://doi.org/10.1007/s10311-021-01225-8

[18] Perna, F. M., Vitale, P., Capriati, V. "Deep eutectic solvents and their applications as green solvents", Current Opinion in Green and Sustainable Chemistry, 21, pp. 27–33, 2020. https://doi.org/10.1016/j.cogsc.2019.09.004

[19] Ahmadzadeh, S., Dolatabadi, M., Malekahmadi, R., Rasooli, A. "Quantum dots and their application in water and wastewater treatment", Journal of Environmental Health and Sustainable Development, 8(1), pp. 1862–1864, 2023. https://doi.org/10.18502/jehsd.v8i1.12317

[20] AlOmar, M. K., Hayyan, M., Alsaadi, M. A., Akib, S., Hayyan, A., Hashim, M. A. "Glycerol-based deep eutectic solvents: Physical properties", Journal of Molecular Liquids, 215, pp. 98–103, 2016. https://doi.org/10.1016/j.molliq.2015.11.032

[21] Smith, E. L., Abbott, A. P., Ryder, K. S. "Deep eutectic solvents (DESs) and their applications", Chemical Reviews, 114(21), pp. 11060–11082, 2014. https://doi.org/10.1021/cr300162p

[22] Abo-Hamad, A., Hayyan, M., AlSaadi, M. A., Mirghani, M. E. S., Hashim, M. A. "Functionalization of carbon nanotubes using eutectic mixtures: A promising route for enhanced aqueous dispersibility and electrochemical activity", Chemical Engineering Journal, 311, pp. 326–339, 2017. https://doi.org/10.1016/j.cej.2016.11.108

[23] Yusuf, J. Y., Soleimani, H., Chuan, L. K., Soleimani, H., Sulaimon, A. A., Balogun, B. B., Adam, A. A., Balogun, A. I. "Eco-friendly functionalization of MWCNTs with deep eutectic solvents", Inorganic Chemistry Communications, 163, 112282, 2024. https://doi.org/10.1016/j.inoche.2024.112282

[24] Pravina, R., Uthayakumar, H., Sivasamy, A. "Hybrid approach based on response surface methodology and artificial neural networks coupled with genetic algorithm (RSM–GA–ANN) for the prediction and optimization of dye photodegradation using nano ZnO anchored glass fiber under solar light irradiation", Journal of the Taiwan Institute of Chemical Engineers, 153, 105248, 2023. https://doi.org/10.1016/j.jtice.2023.105248

[25] Jiang, J., Sandler, S. I., Schenk, M., Smit, B. "Adsorption and separation of linear and branched alkanes on carbon nanotube bundles from configurational-bias Monte Carlo simulation", Physical Review B, 72(4), 045447, 2005. https://doi.org/10.1103/PhysRevB.72.045447

[26] AlOmar, M. K., Alsaadi, M. A., Jassam, T. M., Akib, S., Hashim, M. A. "Novel deep eutectic solvent-functionalized carbon nanotubes adsorbent for mercury removal from water", Journal of Colloid and Interface Science, 497, pp. 413–421, 2017. https://doi.org/10.1016/j.jcis.2017.03.014

[27] Davarnejad, R., Soofi, B., Farghadani, F., Behfar, R. "Ibuprofen removal from a medicinal effluent: A review on the various techniques for medicinal effluents treatment", Environmental Technology & Innovation, 11, pp. 308–320, 2018. https://doi.org/10.1016/j.eti.2018.06.006

[28] Lin, T., Bajpai, V., Ji, T., Dai, L. "Chemistry of carbon nanotubes", Australian Journal of Chemistry, 56(7), pp. 635–651, 2003. https://doi.org/10.1071/CH02254

[29] Li, Y.-H., Wang, S., Luan, Z., Ding, J., Xu, C., Wu, D. "Adsorption of cadmium (II) from aqueous solution by surface oxidized carbon nanotubes", Carbon, 41(5), pp. 1057–1062, 2003. https://doi.org/10.1016/S0008-6223(02)00440-2

[30] Chen, X. "Modeling of experimental adsorption isotherm data", Information, 6(1), pp. 14–22, 2015. https://doi.org/10.3390/info6010014

[31] Makris, D. P., Lalas, S. "Glycerol and glycerol-based deep eutectic mixtures as emerging green solvents for polyphenol extraction: The evidence so far", Molecules, 25(24), 5842, 2020. https://doi.org/10.3390/molecules25245842